3D printed poly(ε-caprolactone) scaffolds function with simvastatin-loaded poly(lactic-co-glycolic acid) microspheres to repair load-bearing segmental bone defects

ZHAN-ZHAO ZHANG*, HUI-ZHONG ZHANG* and ZHI-YONG ZHANG

Shanghai Key Laboratory of Tissue Engineering, Department of Plastic and Reconstructive Surgery, Shanghai Ninth People's Hospital, School of Medicine, Shanghai Jiao Tong University, Shanghai 200011, P.R. China

Received February 1, 2018; Accepted August 9, 2018

DOI: 10.3892/etm.2018.6947

Abstract. Repairing critical-sized bone defects has been a major challenge for orthopedic surgeons in the clinic. The generation of functioning bone tissue scaffolds using osteogenic induction factors is a promising method to facilitate bone healing. In the present study, three-dimensional (3D) printing of a poly(lactic-co-glycolic acid) (PLGA) scaffold with simvastatin (SIM) release functioning was generated by rapid prototyping, which was incorporated with collagen for surface activation, and was finally mixed with SIM-loaded PLGA microspheres. *In vitro* assays with bone marrow-derived mesenchymal stem cells were conducted. For the *in vivo* study, scaffolds were implanted into segmental defects created on the femurs of Sprague-Dawley rats. At 4 and 12 weeks following surgery, X-ray, micro-computed tomography and histological analysis were performed in order to evaluate bone regeneration. The results demonstrated that collagen functionalization of PLGA produced better cell adhesion, while the sustained release of SIM promoted greater cell proliferation with no significant cytotoxicity, compared with the blank PCL scaffold. Furthermore, *in vivo* experiments also confirmed that SIM-loaded scaffolds played a significant role in promoting bone regeneration. In conclusion, the present study successfully manufactured a 3D printing PLGA scaffold with sustained SIM release, which may meet the requirements for bone healing, including good mechanical strength and efficient osteoinduction ability. Thus, the results are indicative of a promising bone substitute to be used in the clinic.

Correspondence to: Dr Zhi-Yong Zhang, Shanghai Key Laboratory of Tissue Engineering, Department of Plastic and Reconstructive Surgery, Shanghai Ninth People's Hospital, School of Medicine, Shanghai Jiao Tong University, 639 Zhizaoju Road, Shanghai 200011, P.R. China
E-mail: doczhiyong@126.com

*Contributed equally

Key words: 3D printing, control release, bone defect, simvastatin, artificial bone, microspheres

Introduction

Bone defects arise following surgery for bone tumors, traumatic injury or congenital disorders, and often require surgical intervention using effective bone grafts. Ideal scaffolds for bone tissue engineering usually require strong mechanical properties as well as good biocompatibility (1), new bone-synchronizing degradation abilities (2,3), adjustable pore structure and osteogenesis-promoting capabilities (4). To date, the most frequently used bone substitute materials include metal, ceramics and natural or synthetic polymers (5). However, metallic scaffolds may weaken bone growth due to stress shielding as a result of excessive rigid fixation, while ceramic is associated with brittleness and poor degradability (6-8). Due to these issues with the current bone repair materials available, further investigation is required in order to identify novel bone tissue engineering scaffolds.

Poly(ε-caprolactone) (PCL) has drawn much attention in the field of bone tissue engineering due to its excellent biocompatibility, biodegradability, mechanical properties and workability (9). However, the major limitations of PCL are that it lacks a cell recognition site and is hydrophobic, thus, it can induce *in vivo* fibrous encapsulation (10). Therefore, a number of previous studies have been performed to investigate methods of enhancing the cell affinity of PCL, such as through surface coating with collagen (11-13).

An ideal bone tissue engineering scaffold should be as similar as possible to the natural bone, which is a type of mineralized collagen composite with hierarchical structure; thus, many previous studies have focused on using biomimetic strategies in order to fabricate scaffolds (5,14,15). As a completely computer aided process, three-dimensional (3D) printing technology, also known as rapid prototyping (RP), provides a new method to accurately design and produce scaffolds with high porosity and connectable pore networks (8,16). In order to build a scaffold that matches the function and structure of natural bone, a hierarchical composite scaffold is constructed by combining the RP technology with the bionic functional manufacturing strategy, as applied in the present study.

Simvastatin (SIM), which is currently used clinically to lower blood cholesterol and low-density lipoprotein, has been hypothesized to promote osteoblast proliferation and differentiation, inhibit osteoclast activity and support immune cells such as macrophages; thus, it has been proposed to enhance bone repair (17-21). A controlled drug release system is able to provide a sustained stimulus for bone regeneration. For this reason, the controlled release of SIM was applied in the present study with poly(lactic-co-glycolic acid) (PLGA) microspheres. Owing to its good biocompatibility and drug-loading properties, PLGA has been approved by the US Food and Drug Administration for application in pharmaceuticals, medical materials and tissue engineering (22). Furthermore, microspheres based on PLGA are of stable degradability and are easy to fabricate since the size and distribution of particles are controllable; they are therefore becoming increasingly favorable as drug carriers (23-26).

In the present study, a PCL macro-porous framework construct was first generated using RP technology, which had favorable mechanical properties to support nascent bone tissue in growth. Then, collagen (COL) incorporating SIM-loaded PLGA microspheres was coated on to the PCL framework using the evacuation method to formulate bone-like microporous networks and to provide a sustained osteoinduction stimulus. The *in vitro* osteogenic effect of the scaffolds was evaluated using bone marrow-derived mesenchymal stem cells (BMSCs), and their *in vivo* osteogenic potential was investigated using a rat femur defect model.

Materials and methods

Materials. PCL was purchased from Shenzhen Esun Industrial Co., Ltd. (Shenzhen, China). COL was purchased from Sichuan Mingrang Bio-Tech Co., Ltd. (Sichuan, China). N-(3-dimethylaminopropyl)-N'-ethylcarbodiimide hydrochloride crystalline (EDC), SIM and PLGA were purchased from Sigma Aldrich (Merck KGaA, Darmstadt, Germany). A Cell Counting Kit-8 (CCK-8) was obtained from Dojindo Molecular Technologies, Inc. (Kumamoto, Japan). Polyvinyl alcohol (PVA) and dichloromethane were purchased from Aladdin Bio-Chem Technology Co., Ltd. (Shanghai, China).

Generation of SIM-loaded PLGA (SIM-PLGA) microspheres. SIM-PLGA microspheres were prepared by utilizing the single emulsion solvent evaporation method, as previously described (27). A total of 460 mg PLGA and 23 mg SIM were dissolved in 6 ml dichloromethane. The mixture was ultrasonically shaken for 30 sec and left standing at room temperature for 30 min. It was then slowly dropped into aqueous solution containing 3% PVA, and stirred for 6 h until it fully solidified into microspheres. Then the microspheres were rinsed three times with deionized water, centrifuged at 300 x g and 4˚C for 10 min, pre-frozen at -80˚C for 2 h and restored following lyophilization for 24 h.

Encapsulation efficiency. The content of SIM in the microspheres was determined using an ultraviolet (UV) spectrophotometer (Beckman Coulter, Inc., Brea, CA, USA) (26,28-30). UV scanning from 100 to 1,000 nm was used to identify the absorption peak of SIM. It was identified that the absorbance of SIM solution was greatly affected by its concentration at 250 nm. The standard absorption curve of SIM was calculated according to the absorbance of samples with known SIM concentrations at 250 nm. The SIM content in the solution was calculated according to the standard absorption curve. Briefly, 1 mg SIM-PLGA microspheres was dissolved in 5 ml acetonitrile and sonicated at 40,000 Hz for 40 sec at room temperature. The UV absorbance of the sample was examined and the concentration of SIM was determined using the standard curve. Encapsulation efficiency of the SIM-PLGA microspheres was calculated according to the following formula: Encapsulation efficiency (%)=(amount of encapsulated SIM)/(amount of total SIM) x100%.

Release properties. A total of 1 mg of PLGA microspheres was incubated with 5 ml PBS and placed in a vibrating screen with constant stirring (60 rpm) at 37˚C. After 1, 3, 7, 14, 21 and 28 days, 2.5 ml of the supernatant was removed and an equal volume of fresh PBS was added. The content of SIM in the solution was quantified using a UV spectrophotometer as aforementioned.

PCL scaffold generation and functionalization. PCL scaffolds were generated with a fused deposition modeling 3D printer (Glarun Technology Co., Ltd., Nanjing, China) as previously described (5). Briefly, a 3D porous CAD model was established and modified in stl format using Magics software 2.1 (Materialise, Leuven, Belgium), processed in the 0-60-120˚ pattern with a filament width of 500 μm, and the final vertical and lateral pore sizes of 1,000 and 250 μm, respectively. The PCL scaffold was then produced according to the stl module. Firstly, the raw PCL material was heated to 120˚C, so that PCL melted to a half flow state. Using the computer controls, according to the shape of the STL file module, PCL with a diameter of 500 μm was squeezed from the nozzle along the X- and Y-axis, cooled to room temperature and allowed to solidify. Then, the nozzle was raised to a specific height along the Z-axis and the process was repeated. The new half flow PCL was squeezed from the nozzle and tightly bound to the lower layer after cooling and solidifying.

Generation of the PCL/COL/SIM-PLGA scaffold. For surface activation, the PCL scaffolds were first alkaline-treated with 5 M NaOH solution at 37˚C for 24 h, and then subsequently immersed in COL solution (1 wt% in 0.1 M acetic acid), vacuumed for 30 min, frozen at -80˚C and freeze-dried at -50˚C for 48 h in order to obtain the preliminary COL-PCL composite. The scaffolds were then cross-linked with 5 mM EDC solution for 24 h, thoroughly washed with 5 wt% glycine solution and distilled water three times, and freeze-dried at -50˚C for 24 h. To incorporate the SIM-PLGA into the PCL/COL scaffolds, 7 mg of microspheres was added to 10 ml COL solution, thoroughly mixed by manual agitation and freeze-dried as aforementioned.

Morphology and porosity observations. The morphologies of the scaffold and the microspheres were observed by field-emission scanning electron microscopy (SEM; Hitachi S-4800; Hitachi, Ltd., Tokyo, Japan) at a beam energy of 10 and 3 keV, respectively. To evaluate the PCL/COL scaffold,

the molded samples were cut into 5x2.5x2.5 mm pieces, which were then gold-coated prior to observation. The porosity of the scaffolds was measured using an ethanol infiltration method. The sample was slowly immersed into a known volume (V_1) of absolute alcohol solution (Aladdin Bio-Chem Technology Co., Ltd.) inside a measuring cylinder. After 1 h, the total volume of alcohol and sample was regarded as V_2. Following careful removal of the sample, the residual volume of alcohol solution was measured as V_3. The results were determined from the following formula: Porosity (%)=$(V_1-V_3)/(V_2-V_3)$ x100%.

In vitro cell seeding, proliferation, viability and cytotoxicity evaluations. BMSCs were obtained from newborn Sprague-Dawley rats as described in a previous study with ethical approval from the Animal Care and Use Committee of Shanghai Ninth People's Hospital (Shanghai, China) (31). The protocol conformed to the National Institutes of Health Guidelines concerning the Care and Use of Laboratory Animals (32). The cell culture medium consisted of 89% Dulbecco's modified Eagle's medium (Invitrogen; Thermo Fisher Scientific, Inc., Waltham, MA, USA), 10% fetal bovine serum (Invitrogen; Thermo Fisher Scientific, Inc.) and 1% penicillin-streptomycin (Invitrogen; Thermo Fisher Scientific, Inc.). Passages 2-3 of BMSCs w ere used for the subsequent experiments.

For evaluation of cell-seeding efficiency, $5x10^5$ cells in 100 μl D10 medium were added into the constructs (PCL, PCL/COL and PCL/COL/SIM-PLGA; n=5 each group). The cell number was counted as W_1. Following incubation for 4 h, the seeded constructs were removed and washed with PBS. Cells that had adhered were digested with trypsin and were counted as W_2; thus, the cell seeding efficiency was calculated according to the following formula: Cell seeding efficiency=W_2/W_1.

To evaluate cytotoxicity, $1x10^3$ BMSCs were seeded onto a 96-well plate and incubated for 4 h in D10 medium, then the medium was replaced with fresh medium, fresh D10 medium with 5% DMSO, or the extract fluid of PCL, PCL/COL, or PCL/COL/SIM-PLGA, which was prepared by immersing the constructs in D10 medium for 72 h (n=5). CCK-8 assays were then performed to assess the cytotoxicity 1 day later at a wavelength of 450 nm.

To evaluate cell proliferation, $3x10^4$ cells in 20 μl D10 medium were seeded into the PCL, PCL/COL, PCL/COL/SIM-PLGA, or decalcified bone matrix (DBM; cut to 5x2.5x2.5 mm) in 24-well plates and incubated in 1 ml of D10 medium for 1 h. The procedure was then repeated on the other side of the constructs. At 1, 3 and 7 days after seeding, cell proliferation on the different constructs was assessed by CCK-8 assay. DBM was prepared as described in a previous study (33).

Alkaline phosphatase (ALP) and Alizarin red staining. Since it is difficult to extract the mRNA of cells directly cultured on scaffolds, and the blank scaffold would have very poor osteoinduction since this property is primarily due to the encapsulated drug, cells were cultured on the well plate and scaffolds were placed on the Transwell membrane above the cells (34). BMSCs ($1x10^4$) of passage 3 were seeded in 24-well plates. After 6 h, 1 ml of osteogenic induction medium (50 mg/ml ascorbic acid, 10 mM β-glycerophosphate and 10 nM dexamethasone) was added. Then, the 0.8-μm-pore inserts and the different scaffolds were added to the wells of the culture plates. On day 7 following osteogenic induction, the cells were fixed in 4% paraformaldehyde for 20 min at room temperature and stained in ALP staining solution (Beyotime Institute of Biotechnology, Haimen, China) at 37˚C for 10 min in the dark. ALP activity after 7 and 14 days of culture was quantified using the QuantiChrom™ Alkaline Phosphatase Assay kit (BioAssay Systems; Thermo Fisher Scientific, Inc.), and the total protein content was assessed with a BCA Protein Assay kit (Thermo Fisher Scientific, Inc.). The mineralized matrix nodules formed by BMSCs were evaluated using Alizarin red staining. On day 21, the cells were washed three times with PBS, fixed in 4% paraformaldehyde at room temperature for 30 min and incubated with Alizarin red solution (Beyotime Institute of Biotechnology) for 10 min at room temperature. To quantify the levels of mineralization, the mineralized matrix nodules were dissolved in 10% (w/v) cetylpyridinium chloride (Aladdin Bio-Chem Technology Co., Ltd.) and the absorbance was measured at 450 nm using a microplate reader.

Reverse transcription-quantitative polymerase chain reaction (RT-qPCR). The expression of genes associated with osteogenesis was assessed by RT-qPCR, as previously described (35). After 7 and 14 days of culture, total RNA was prepared using TRIzol reagent (Invitrogen; Thermo Fisher Scientific, Inc.) in order to determine the mRNA expression of ALP and COL type 1 (COL 1), which are associated with osteogenesis. cDNA was obtained by reverse transcription at 37˚C for 1 h using BeyoRT™ II First Strand cDNA Synthesis kit with gDNA Eraser (Beyotime Institute of Biotechnology) from 1 μg RNA and stored at -20˚C. qPCR was conducted using SYBR GreenER qPCR SuperMix reagents (Invitrogen; Thermo Fisher Scientific, Inc.). The following thermocycling conditions were used for the PCR: Initial denaturation at 95˚C for 10 min; 30 cycles of 95˚C for 15 sec, and 60˚C for 1 min; and a final dissociation cycle at 95˚C for 15 sec, 60˚C for 1 min and 95˚C for 15 sec. The following 5'-3' primer sequences were used: ALP forward, CGTGGAAACCTGATGTATGCT and reverse, ACTCCTATGACTTCTGCGTCTG; COL 1 forward, GAAAGAGAAAGACCCCAGTTAC and reverse, ATACCA TCTCCCAGGAACAT; β-actin forward, CCTCTATGCCAA CACAGT and reverse, AGCCACCAATCCACACAG; BSP forward, GATAGTTCGGAGGAGGAGGG and reverse, CTA ACTCCAACTTTCCAGCGT; OPN forward CCTGGACCT CATCAGCATTT and reverse TTGGAGCAAGGAGAACCC; RUNX2 forward GCACCCAGCCCATAATAGA and reverse GACGGTTATGGTCAAGGTGAA; OCN forward GGA GGGCAGTAAGGTGGTGAA and reverse GAAGCCAAT GTGGTCCGCTA. β-actin forward CACGAAACTACCTTC AACTCC and reverse CATACTCCTGCTTGCTGATC. The $2^{-\Delta\Delta Cq}$ method was used to calculate the relative expression of each target gene against the β-actin (36).

In vivo study of segmental defect repair on rat femurs. The following animal experiments were performed with ethical approval from the Animal Care and Use Committee of Shanghai Ninth People's Hospital (Shanghai, China), and conformed to the National Institutes of Health Guidelines concerning the Care and Use of Laboratory Animals (37).

A diagram of the experimental procedure is presented in Fig. 1. A total of 12 male Sprague-Dawley rats aged 6-8 weeks (~200 g) were purchased from the Shanghai Jiao Tong University Research Center of Laboratory Animal (Shanghai, China). The animals were housed and acclimatized at the experimental animal laboratory of Shanghai Ninth People's Hospital (Shanghai, China) under controlled temperature (25˚C) and humidity (55%) with a 12-h light/dark cycle, with free access to food and water. The rats were randomly divided into three groups: i) PCL (bone defect + blank PCL scaffold); ii) PCL/COL (bone defect + PCL scaffold coated with COL); and iii) PCL/COL/SIM-PLGA (bone defect + PCL scaffold coated with COL and SIM-loaded PLGA microspheres; n=4 each group). Rats were anesthetized via intraperitoneal injection of 1% pentobarbital sodium (Invitrogen; Thermo Fisher Scientific, Inc.; 40 mg/kg). Under a standard surgical procedure, the femur was fully exposed and holes were made on both femoral ends with a micro bone drill. Then, a titanium plate (15x2.8 mm) was fixed along the femur using tapping screws (1 mm in diameter, 6 mm in length). Then, a 5 mm-long segmental defect was made in the middle position corresponding to the plate with the bone drill, which was then cleaned with 0.9% saline and the PCL, PCL/COL and PCL/COL/SIM-PLGA scaffolds were transferred to the defect area respectively.

X-ray examination was performed at 4 and 12 weeks after surgery. At 12 weeks post-surgery, the animals were sacrificed and the femurs of rats were fixed in 4% paraformaldehyde at room temperature for a week. The specimens were then detected by micro-computed tomography (micro-CT; SCANCO μ-80 Micro-CT; SCANCO Medical AG, Brüttisellen, Switzerland). 3D reconstruction and calculation of the new bone tissue was subsequently performed with the built-in micro-CT software. The regions of interest were restricted to the cylindrical part covering the defect, whereas regions with CT values of 1,300-3,500 were determined as bone tissue.

Histological assay. Following micro-CT testing, the specimens were decalcified with 10% EDTA, dehydrated, paraffin embedded, sectioned into 5-μm-thick slices for hematoxylin and eosin (HE; 30 min at room temperature) and Masson trichrome (20 min at room temperature) staining, and examined by light microscopy.

For immunohistochemistry, the sections were blocked with 5% bovine serum albumin (Invitrogen; Thermo Fisher Scientific, Inc.) for 30 min at room temperature and then incubated with the anti-osteocalcin (OCN; Abcam, Cambridge, UK; cat. no. ab198228; 1:200) primary antibody overnight at room temperature. The sections were then incubated with the horseradish peroxidase-conjugated goat anti-rabbit IgG (H+L) secondary antibody (Beyotime Institute of Biotechnology; cat. no. A0208) at a dilution of 1:200 for 1 h at room temperature, visualized with 3,3-diaminobenzidine solution, and counter-stained with hematoxylin (Beyotime Institute of Biotechnology) for 1 h at room temperature. Image Pro Plus software 6.0 (Media Cybernetics, Inc., Rockville, MD, USA) was used to analyze the results.

Statistical analysis. All data are expressed as the mean ± standard deviation. The results were evaluated by one-way analysis of variance with Tukey's post-hoc using SPSS 15.0 software for Windows (SPSS, Inc., Chicago, IL, USA). $P<0.05$ was considered to indicate a statistically significant difference.

Results

Surface characterization. As demonstrated in the SEM images, the SIM-PLGA microspheres assumed a configuration with a smooth, glossy surface and regular spherical shape (Fig. 2A), indicating that the experimental conditions for the manufacture of microspheres were stable and suitable (31,38,39). The particle diameter (Fig. 2B) ranged from 2-20 μm (mean, 12.11 μm). The narrow particle size distribution suggested that the drug release from scaffolds would be relatively stable (40,41). In addition, the encapsulation efficiency of SIM inside the PLGA microspheres reached ~86.3%. An initial outbreak release was detected in the first 3 days. As indicated in the *in vitro* release diagram, ~40% of the primarily integrated SIM was leaked from the PLGA microspheres within the first 3 days, which was followed by sustained release over 27 days (Fig. 2C). At the end of the release assay, almost 90% of the SIM-loaded microspheres were released (Fig. 2C), and the cumulative drug release achieved ~86.9%.

In the present study, the PCL scaffold alone exhibited a vertical aperture at 917±14.8 μm. Porous COL with good biological activity was well compounded onto the PCL scaffold by vacuuming and freeze-drying, forming a thin coating layer. COL displayed porosity with homogeneous pore sizes, filling in the horizontal pores in a reticular pattern and covering the trabecula of the PCL scaffold. Therefore, the PCL/COL composite possessed a two-level pore structure, consisting of macro-porous PCL (~1,000 μm) and microporous COL (~100 μm). Following further incorporation, PLGA microspheres were evenly distributed in the COL network (Fig. 3A). The pore size of PCL/COL was 126.7±18.42 μm, whereas that of PCL/COL/SIM-PLGA was 125.7±15.82 μm (Fig. 3B). In addition, the porosity of the three constructs was 59.05±1.7, 57.5±0.1 and 57.4±0.1%, respectively (Fig. 3C). These results revealed that a reduced but hierarchical structure was formed following COL modification, while the incorporation of SIM-PLGA had no significant effect on porosity.

In vitro cellular evaluation

Cell proliferation and viability. BMSCs were directly seeded on the scaffold. The cell-seeding efficiency was revealed to be 54±2.2% for PCL, 88.6±2.0% for PCL/COL and 89±1.6% for PCL/COL/SIM-PLGA. PCL/COL and PCL/COL/SIM-PLGA exhibited a significantly higher efficiency (1.64- and 1.65-fold increase, respectively) when compared with PCL alone (Fig. 4A). The improvement in cell seeding may be attributable to the greater contact area with the COL network and more adhesion sites from the COL matrix, while PLGA microspheres may have exerted little influence. The extracted fluid test demonstrated that there was no significant cytotoxicity in the scaffolds when compared with the untreated BMSC group, indicating that no toxic substances were identified during the COL cross-linking process, and thus demonstrating its biosafety (Fig. 4B). Furthermore, the greatest levels of proliferation were produced by the SIM-PLGA group, which may be caused by the SIM released from the scaffold (Fig. 4C).

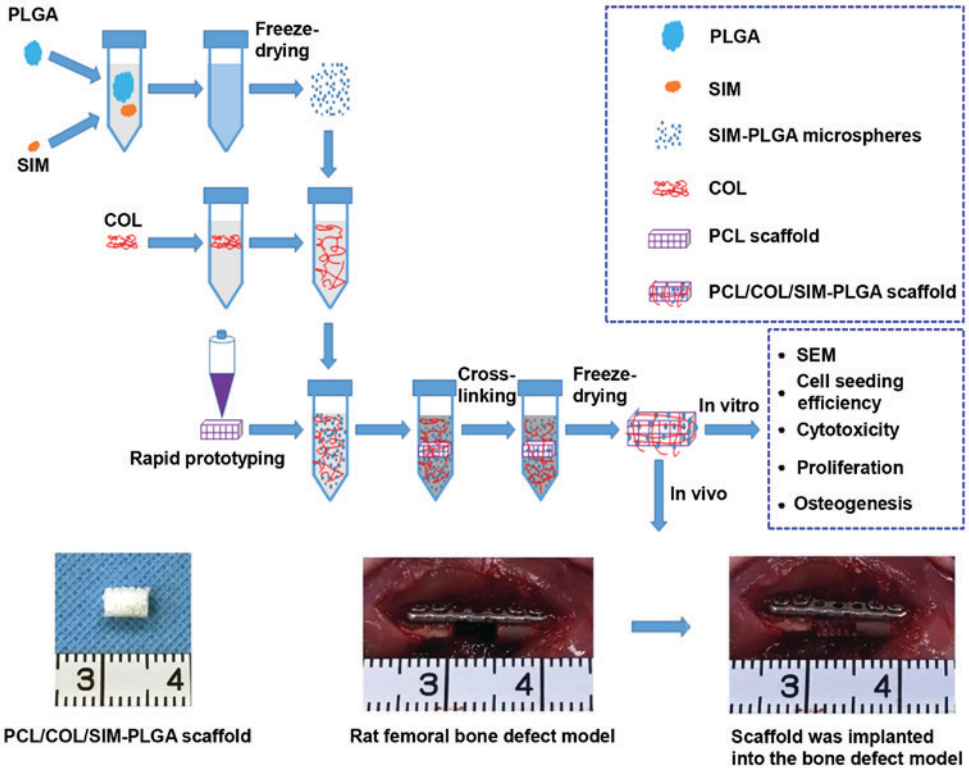

Figure 1. Flow chart depicting the sequence of experiments conducted in the present study. The mixture of PLGA and SIM was ultrasonically shaken for 30 sec and stirred in 3% polyvinyl alcohol for 6 h until it fully solidified into microspheres. The microspheres were lyophilized for 24 h and added to COL solution, then thoroughly mixed by manual agitation. Subsequently, PCL scaffold was immersed in the mixture of COL and microspheres, cross-linked with 5 mM N-(3-dimethylaminopropyl)-N'-ethylcarbodiimide hydrochloride crystalline solution for 24 h and freeze-dried for 48 h. The bioactivity of the scaffold was tested both *in vitro* and *in vivo*. PLGA, poly(lactic-co-glycolic acid); SIM, simvastatin; COL, collagen; PCL, poly(ε-caprolactone); SEM, scanning electron microscopy.

Osteogenic potency of BMSCs. To assess the osteogenic potency of BMSCs treated with the different constructs, the present study performed Alizarin red and ALP staining. Cells were cultured on the well plate and scaffolds were placed on a Transwell membrane above the cells. Typical osteogenic differentiation was observed in all three groups. However, the SIM/PLGA group exhibited higher ALP activity and more mineralized nodules (Fig. 5A). Despite the increase in ALP expression noted in all three groups following 14 days of differentiation when compared with that observed after 7 days (Fig. 5B), the SIM-PLGA group exhibited significantly higher expression levels when compared with the other three groups at 7 and 14 days. Furthermore, quantitative analysis of Alizarin red staining indicated that the OD value of the SIM/PLGA group was the highest among the four groups, suggesting that the mineral deposition and the osteogenic differentiation of BMSCs improved. By contrast, the DBM group exhibited similar osteogenesis to the PCL group, as determined by the quantitative results of Alizarin red staining (Fig. 5C).

Osteogenic gene expression. RT-qPCR was performed to examine the mRNA levels of ALP, bone sialoprotein, COL 1, runt-related transcription factor 2, osteopontin and OCN in the BMSCs of the different groups. As presented in Fig. 6, the SIM-PLGA group exhibited significantly higher expression levels of all osteogenic genes when compared with the other groups at days 7 and 14.

In vivo study of rat femur defects

X-ray and micro-CT examination. As indicated in Fig. 7A, at 4 weeks post-surgery, the X-ray images revealed that the PCL group exhibited only a small amount of bone tissue growth, with no significant increase in bone deposition at 12 weeks and no bone fracture healing. On the other hand, significant levels of bone tissue growth were observed at 4 weeks in the PCL/COL and PCL/COL/SIM-PLGA groups. Notably, complete defect repair with continuous cortical bone was achieved in the PCL/COL/SIM-PLGA group at 12 weeks post-implantation. The results of micro-CT demonstrated that there was scattered bone tissue near the defect edges as opposed to obvious newly formed bone in the PCL group. As shown in the 3D reconstructed images, new bone formation reconnected the fractured ends, with the newly formed cortical bone enveloping the scaffolds. Both the PCL/COL and PCL/COL/SIM-PLGA attained improved results compared with the PCL group, and the incorporation of SIM-PLGA further enhanced the osteogenic ability of the PCL/COL scaffolds. Furthermore, the new bone volume calculated according to the 3D reconstructed images indicated that the PCL/COL/SIM-PLGA group exhibited the best bone regeneration among the three groups (Fig. 7B).

Histological qualitative and quantitative analysis. The HE staining results revealed that the defect area was filled with loose fibrous connective tissue, which was stained a light red, and was wrapped around the PCL trabecula (Fig. 8A).

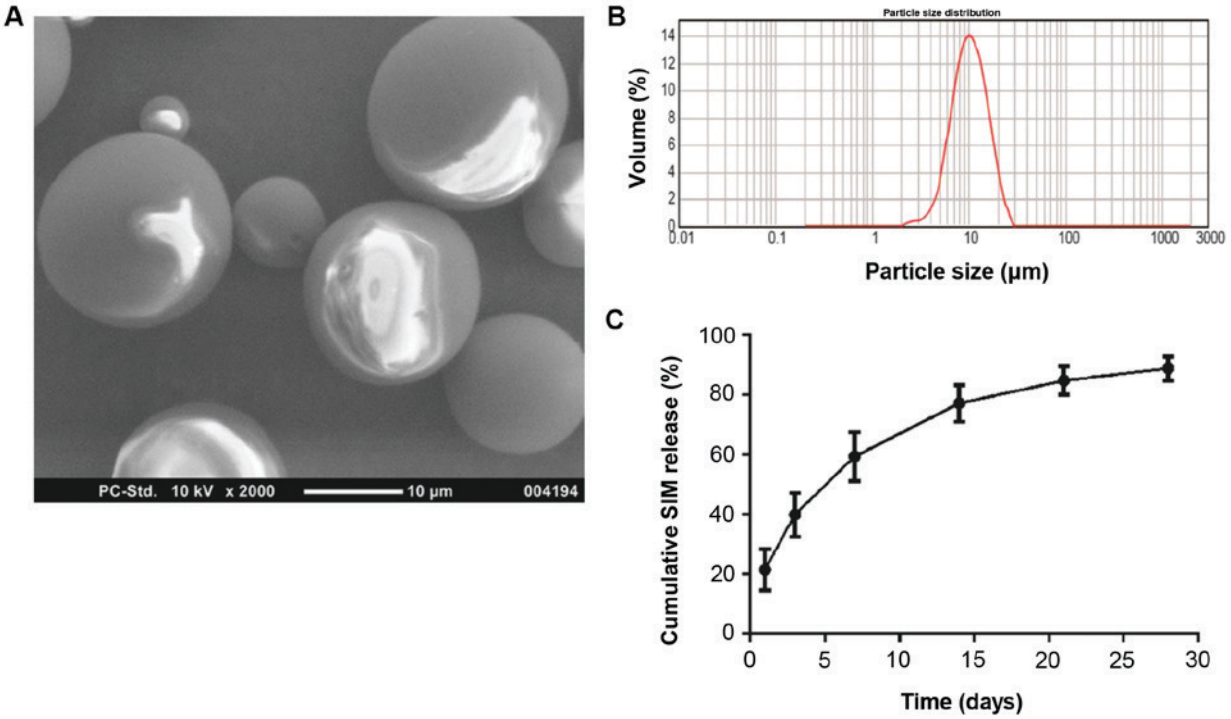

Figure 2. Characteristics of SIM-loaded microspheres. (A) Blank SIM-PLGA microspheres exhibited smooth and round morphology. (B) Particle size distribution of the blank SIM-PLGA microspheres was in the range of 2-30 μm. (C) Cumulative *in vitro* release profile of SIM from PLGA microspheres. PLGA, poly(lactic-co-glycolic acid); SIM, simvastatin.

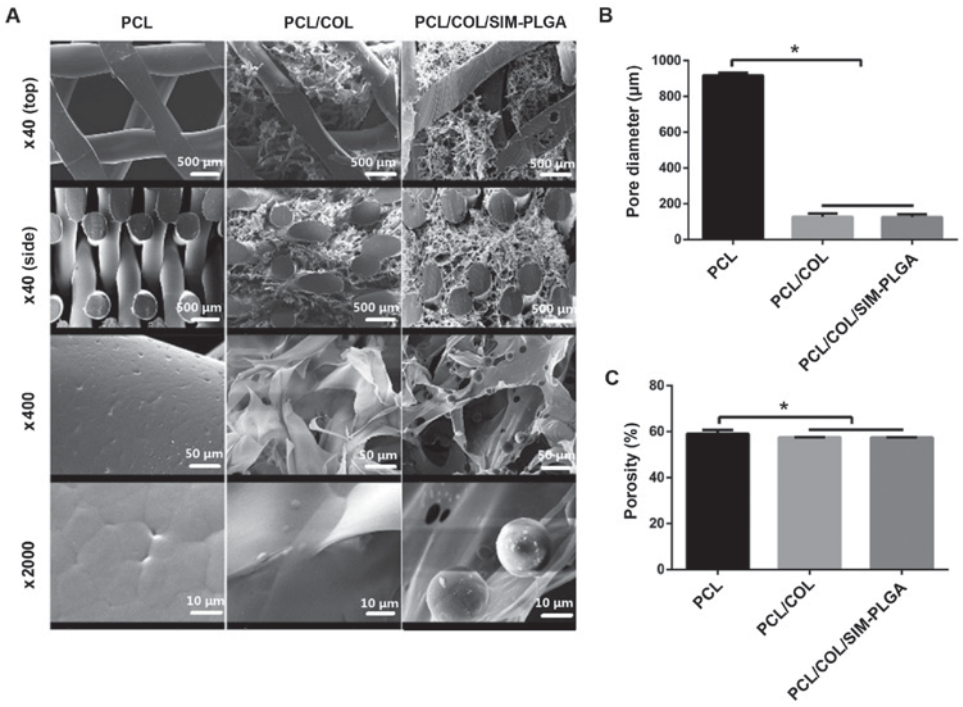

Figure 3. Scanning electron microscopy images of the constructs. (A) PCL frameworks exhibited macroporous (~1,000 μm) architectures with complete interconnectivity. In the COL-modified PCL scaffold (PCL/COL), microporous (126.2±18.42 μm) COL networks homogeneously occupied the voids of the framework and covered the trabecula of the PCL scaffold. PLGA microspheres were evenly distributed in the COL of the PCL/COL/SIM-PLGA scaffold, with minor only effects on the pore structure and porosity. Summary of (B) pore structure and (C) porosity. *P<0.05, as indicated. PLGA, poly (lactic-co-glycolic acid); SIM, simvastatin; COL, collagen; PCL, poly(ε-caprolactone).

The results of Masson trichrome staining were in accordance with that of HE, as the fibrous tissue, stained a light blue, surrounded the scaffolds forming a fibrous interface at the scaffold-bone juncture. In the PCL/COL group, only a marginal amount of fibrous tissue formed, and the defect was filled mostly with newly formed bone tissue; both

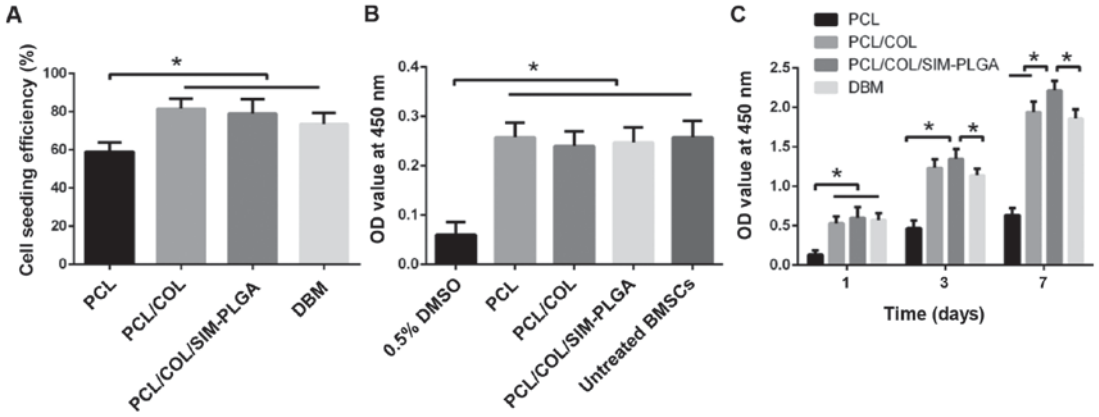

Figure 4. *In vitro* cellular evaluation of the PCL/COL/SIM-PLGA composite constructs. (A) Cell seeding efficiency assay. (B) Cytotoxicity evaluation of the extracted liquid of the scaffolds. (C) Level of cell proliferation in the scaffolds. The PCL/COL/SIM-PLGA scaffold possessed the greatest biocompatibility and exhibited more favorable biological properties, achieving better cellular adhesion and proliferation capacities. *P<0.05, as indicated. PLGA, poly(lactic-co-glycolic acid); SIM, simvastatin; COL, collagen; PCL, poly(ε-caprolactone), DBM, decalcified bone matrix; OD, optical density.

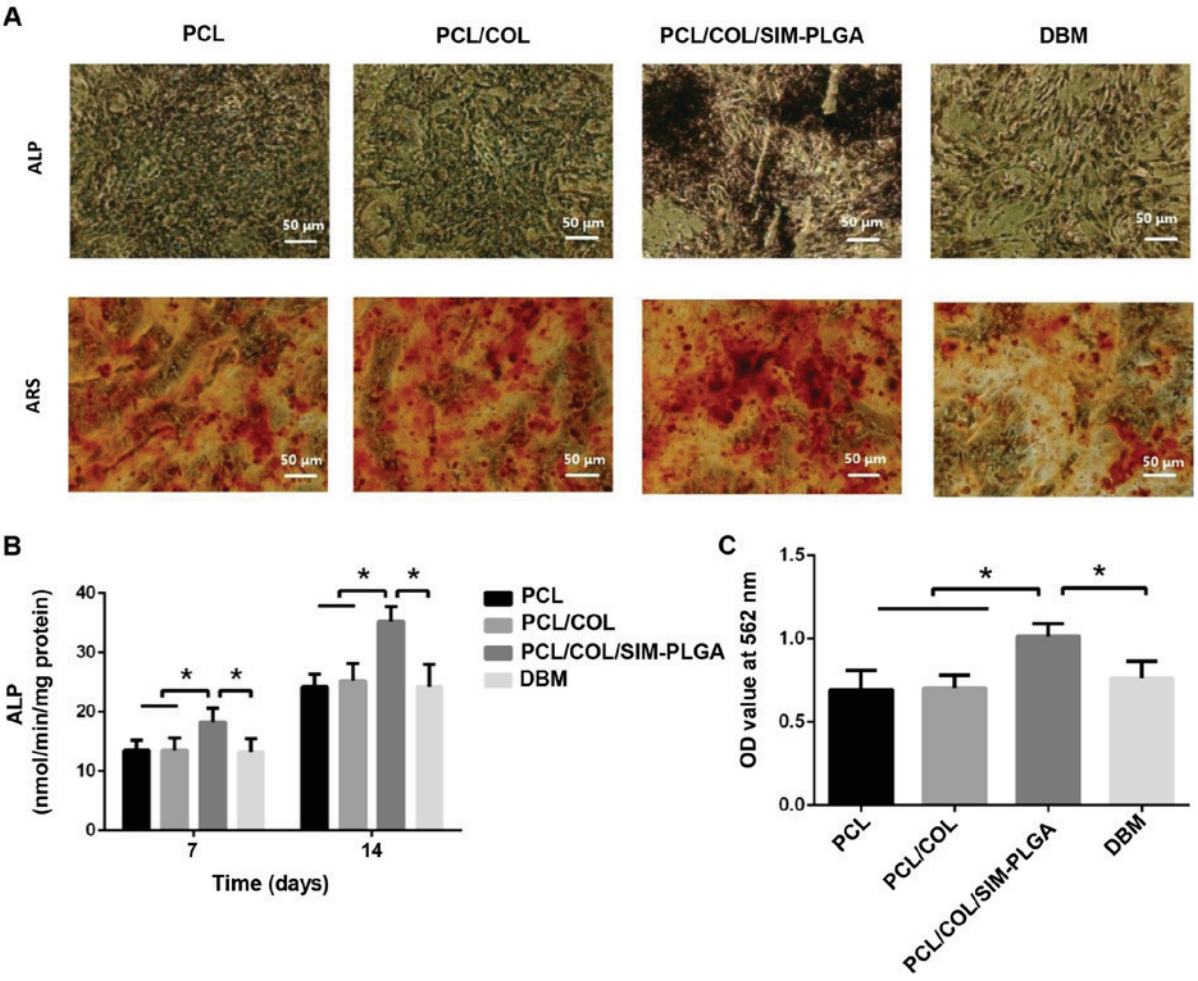

Figure 5. Early and late stages of BMSC osteogenic differentiation, as determined by ALP staining and ARS, respectively. (A) Representative images of ALP staining after 14-day culture and ARS after 21-day culture. (B) ALP activity results. (C) Summary of ARS results. The PCL/COL/SIM-PLGA construct significantly promoted the osteogenic differentiation of BMSCs in both the early and late stages. *P<0.05, as indicated. PLGA, poly(lactic-co-glycolic acid); SIM, simvastatin; COL, collagen; PCL, poly(ε-caprolactone); BMSC, bone marrow-derived mesenchymal stem cells; ALP, alkaline phosphatase; ARS, Alizarin red staining; OD, optical density.

mature (dark blue) and immature (light blue) bone tissue was observed. In the PCL/COL/SIM-PLGA composite scaffold group, the bone tissue in the bone defect was further improved, and was primarily composed of mature bone tissue stained a dark blue. The new bone tissue directly integrated with the scaffold material by connecting with the original bone tissue

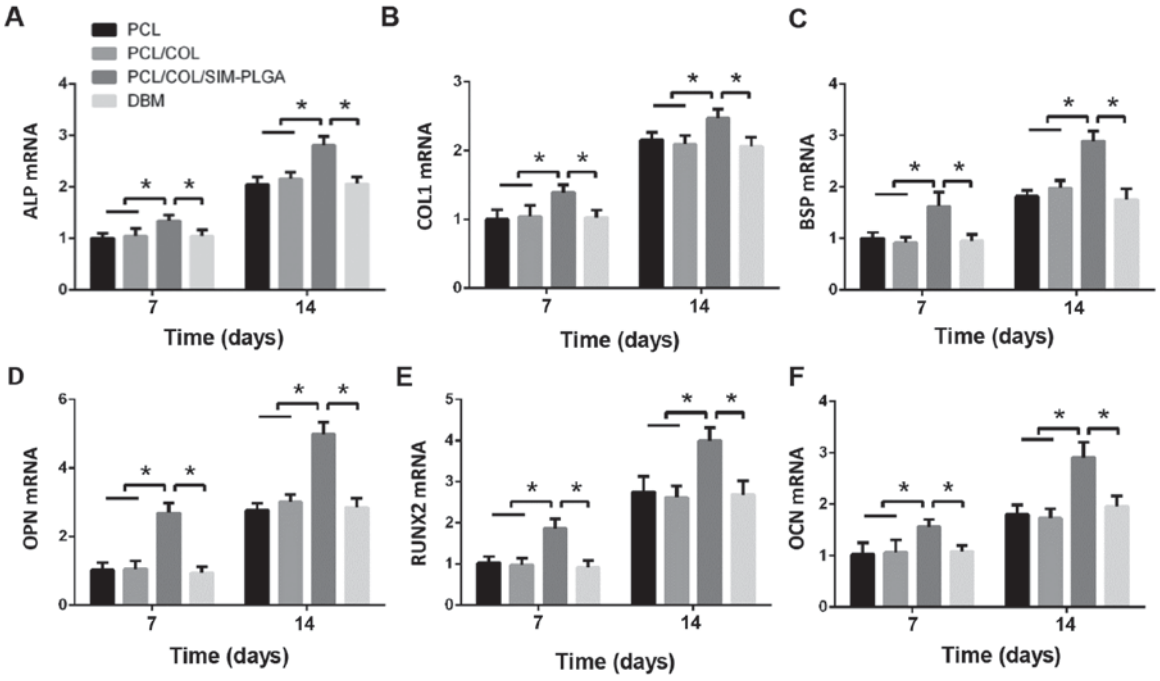

Figure 6. Gene expression analyses of (A) ALP, (B) COL 1, (C) BSP, (D) OPN, (E) RUNX2 and (F) OCN in the different groups after 7 and 14 days of culture. The results are presented as relative ratios to the PCL group at day 7. The expression of osteogenic genes was greatly enhanced by the PCL/COL/SIM-PLGA scaffold. *P<0.05, as indicated. PLGA, poly(lactic-co-glycolic acid); SIM, simvastatin; COL, collagen; PCL, poly(ε-caprolactone); ALP, alkaline phosphatase; COL 1, collagen type 1; BSP, bone sialoprotein; RUNX2, runt-related transcription factor 2; OPN, osteopontin; OCN, osteocalcin.

at the fracture end, which was consistent with the results of micro-CT. Thus, the PCL/COL/SIM-PLGA construct served well in osteogenesis. In addition, quantitative analysis of new bone area also indicated that the PCL/COL exhibited an improved osteoinduction ability compared with the blank PLC scaffold and the PCL/COL/SIM-PLGA scaffold exhibited the highest new bone area among the three groups.

Immunohistochemical staining of OCN. The immunohistochemical staining results (Fig. 9) demonstrated that the PCL/COL/SIM-PLGA group exhibited significantly higher OCN expression compared with the PCL/COL group, as determined by the number of OCN-positive areas (indicated by brown staining). In addition, the level of OCN expression in the PCL/COL and PCL/COL/SIM-PLGA groups was significantly increased compared with the PCL group, which suggested that the composited PCL possessed improved osteogenic ability, with collagen facilitating the PCL to form bone tissue and SIM-PLGA promoting further osteogenesis.

Discussion

In order to accelerate bone reconstruction, an optimal bone implant for clinical practice requires both a porous structure and optimal biocompatibility. The present study employed hybrid 3D PCL scaffolds consisting of PCL, COL and SIM/PLGA, and the results revealed two key points. Firstly, the low degradation rate of the PCL scaffold with an interconnected porous structure provided good mechanical strength and allowed for the delivery of nutrients through the scaffolds. COL modification produced scaffolds with macro/micro hierarchical structures where cells attached and proliferated well among the COL RGD (Arg-Gly-Asp motif) domains and integrin receptors (13). Secondly, the scaffolds conferred high absorbability to the SIM-PLGA microspheres, enhancing osteogenesis and the osteointegration of biomimetic PCL/COL scaffolds.

In our previous study, PCL frames that were incorporated with a COL scaffold significantly increased the surface area and bulk modulus, making best use of the advantages, and bypassing the disadvantages, of using scaffold materials (5). In the present study, in order to further improve the biological functionalities of the composite, SIM-PLGA was subsequently incorporated into the COL scaffold in order to achieve controlled SIM discharge. To elucidate the impact of SIM-PLGA incorporation, the pore size, release diagram, mechanical structure of the scaffolds, cell activity and *in vivo* bone restoration effect were measured.

As indicated in previous research, SIM enhances bone formation by reducing apoptosis and increasing osteogenesis in MSCs (21), as well as inhibiting bone resorption by suppressing the proliferation and differentiation of osteoclasts (42). In the present study, it was also observed that SIM could augment the proliferative and differentiative capabilities of BMSCs, indicating its potential as a bone regenerative molecule. This was also confirmed by the superior osteogenesis elicited by the incorporation of SIM-PLGA in femur bone defect repair. However, it remains difficult to systemically manipulate the uptake of SIM due to its poor drug absorptivity. On the other hand, sufficient doses via local injection may cause inflammation (15). To improve the efficacy of SIM and circumvent its side effects, the present study selected PLGA microspheres as a drug vehicle due to their agreeable biocompatibility, low toxicity and controllable rate of degradation (24,25,43). Sustained release of

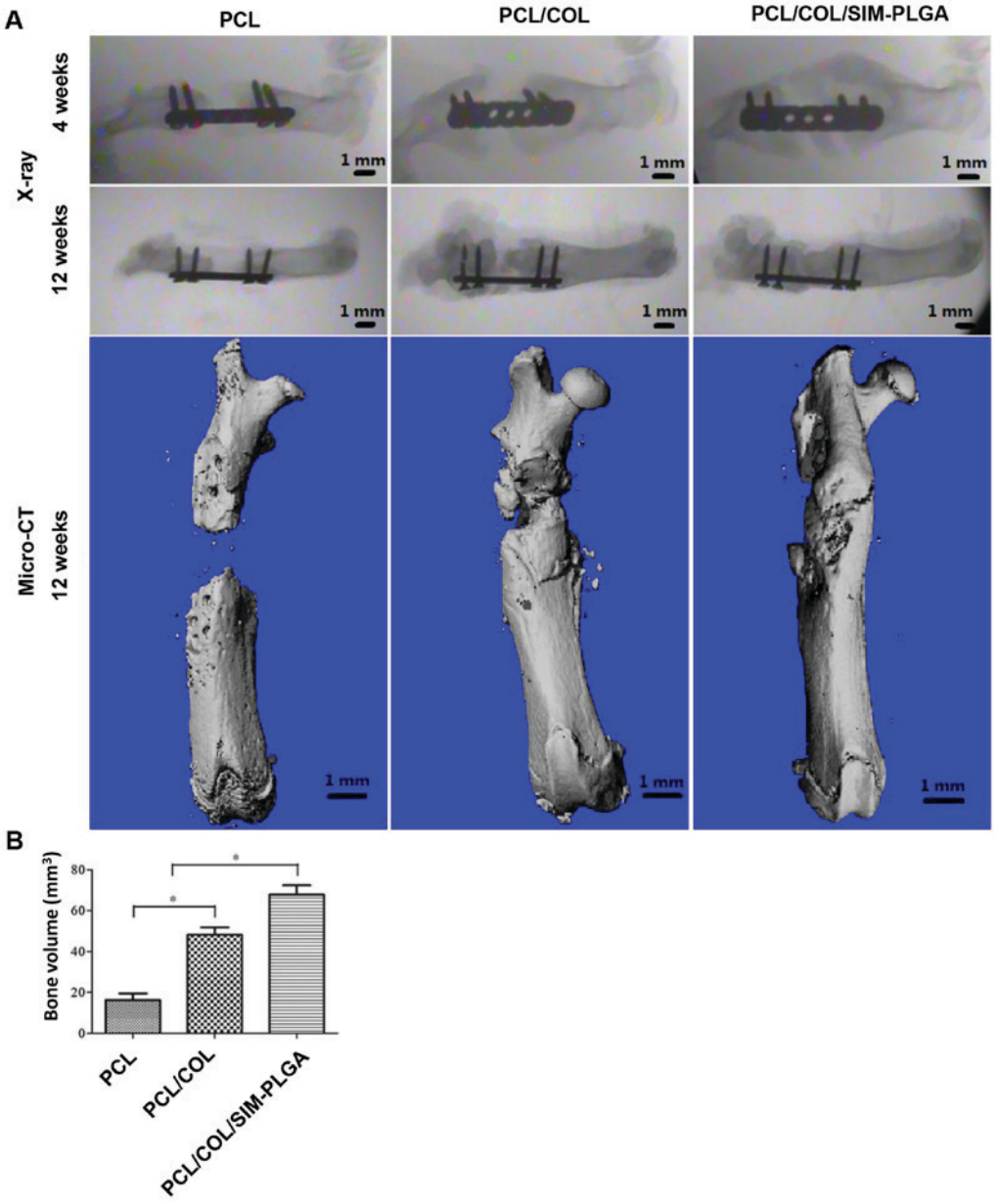

Figure 7. Analysis of bone regeneration of the femur defect with the implanted scaffolds using X-ray and micro-CT. (A) Plain X-ray images of the femur defects at 4 and 12 weeks after transplantation with PCL, PCL/COL or PCL/COL/SIM-PLGA. Micro-CT scan of the femur bone defect at 3 months after surgery. (B) Bone volume. The rats in the PCL/COL/SIM-PLGA group exhibited improved bone repair when compared with the other groups. *P<0.05, as indicated. PLGA, poly(lactic-co-glycolic acid); SIM, simvastatin; COL, collagen; PCL, poly(ε-caprolactone); CT, computed tomography.

SIM plays an essential role in bone regeneration, as a release time of 2-3 weeks is required for growth factors to fulfill ideal bone repair (44). As demonstrated in the release diagram, the release of SIM from the PLGA microspheres lasted >27 days, indicating that PLGA microspheres may serve as appropriate carriers for growth factors.

Porosity is an important determinant of optimal regenerative materials (45). Osteochondral formation usually occurs in pores of a small size; and non-chondral osteogenesis is usually present in pores of a larger size (46,47). Based on previous work (5), the present study fabricated scaffolds with a pore size of 1,000 μm through 3D printing. To simulate the anatomic constitution of human cancellous bone, COL was combined with the PCL scaffold via dry-freezing, thereby acquiring a hierarchical porous structure with a saturated void space (48). Within the COL network, the PLGA microspheres exhibited homogeneous distribution with the pore size slightly diminished.

Since bones function as load-bearing parts, the materials for bone implants must retain strong mechanical properties in order to secure all of the osteogenic cells with sufficient space for tissue regeneration. Due to its good mechanical strength and low rate of degradation, PCL is widely considered to be an appropriate candidate for osteogenic scaffolds. Previous studies have revealed that the compressive strength and modulus of PCL, with a hierarchical pore structure, is similar to that of human cancellous bone (1,49) and could be utilized for bone tissue engineering (1,4), as demonstrated by the present study.

In conclusion, the results of the present study provide the basis for a new strategy for bone tissue regeneration, which incorporates polyesters and biomolecules, forming

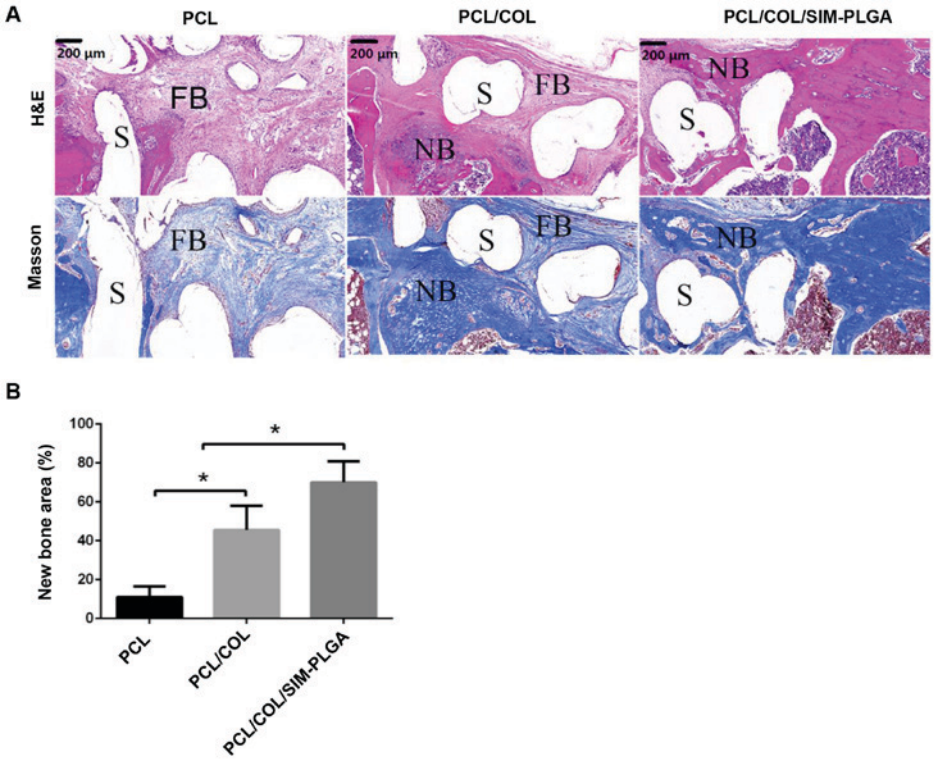

Figure 8. Analysis of bone regeneration of the femur defect by using HE and Masson staining. (A) HE and Masson stained tissue sections of bone regeneration in the defect areas, implanted with PCL, PCL/COL or PCL/COL/SIM-PLGA constructs, at 3 months after surgery. (B) The SIM-loaded scaffold demonstrated the most robust osteogenic activity, and the majority of the defect area in the SIM-loaded scaffold group was filled with eosin-stained newly formed bone tissue. *P<0.05, as indicated. S, scaffolds; NB, newly formed bone; FB, fibrosis; PLGA, poly(lactic-co-glycolic acid); SIM, simvastatin; COL, collagen; PCL, poly(ε-caprolactone); HE, hematoxylin and eosin.

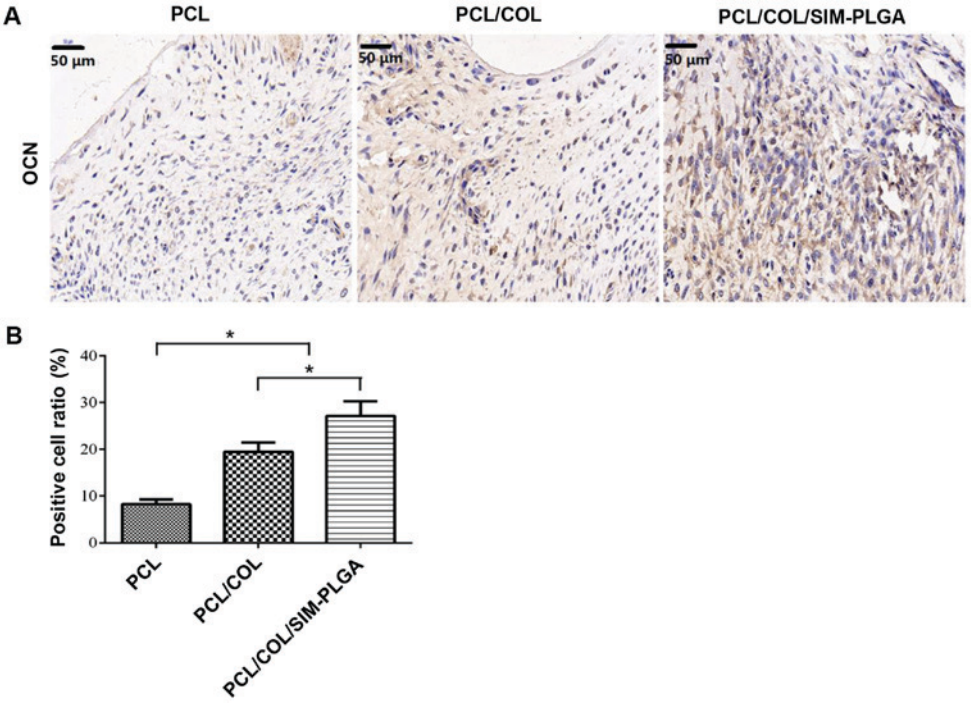

Figure 9. Expression of OCN in the defect area. (A) Representative images of immunohistochemical staining of OCN. (B) Percentage of positively stained cells per field of view was calculated. The PCL/COL/SIM-PLGA group exhibited the greatest levels of OCN staining. *P<0.05, as indicated. PLGA, poly(lactic-co-glycolic acid); SIM, simvastatin; COL, collagen; PCL, poly(ε-caprolactone); OCN, osteocalcin.

a hierarchical structure containing a PCL scaffold of a macro-scale filled with micro-sized COL. With the sustained release of SIM, the present study obtained superior bone formation with sufficient mechanical strength.

Acknowledgements

The authors would like to thank Dr Jinbing Wang and Dr Yu Li (Shanghai Key Laboratory of Tissue Engineering, Department of Plastic and Reconstructive Surgery, Shanghai Ninth People's Hospital, School of Medicine, Shanghai Jiao Tong University, Shanghai, China) for their help in the preparation of the scaffolds.

Funding

No funding was received.

Availability of data and materials

The datasets used and/or analyzed during the present study are available from the corresponding author on reasonable request.

Authors' contributions

The final version of the manuscript has been read and approved by all authors, and each author believes that the manuscript represents honest work. ZZZ and HZZ collaborated to design the study. ZZZ was responsible for experiments. ZZZ and ZYZ analyzed the data. All authors collaborated to interpret results and prepare the manuscript.

Ethics approval and consent to participate

All procedures performed in the current study were approved by the Ethics Committee of Shanghai Ninth People's Hospital.

Patient consent for publication

Not applicable.

Competing interests

The authors declare that they have no competing interests.

References

1. Weisgerber DW, Erning K, Flanagan CL, Hollister SJ and Harley BAC: Evaluation of multi-scale mineralized collagen-polycaprolactone composites for bone tissue engineering. J Mech Behav Biomed Mater 61: 318-327, 2016.
2. Kasuya A, Sobajima S and Kinoshita M: In vivo degradation and new bone formation of calcium phosphate cement-gelatin powder composite related to macroporosity after in situ gelatin degradation. J Orthop Res 30: 1103-1111, 2012.
3. Zhang J, Wang L, Zhang W, Zhang M and Luo ZP: Synchronization of calcium sulphate cement degradation and new bone formation is improved by external mechanical regulation. J Orthop Res 33: 685-691, 2015.
4. Li L, Zuo Y, Zou Q, Yang B, Lin L, Li J and Li Y: Hierarchical structure and mechanical improvement of an n-HA/GCO-PU composite scaffold for bone regeneration. ACS Appl Mater Interfaces 7: 22618-22629, 2015.
5. Wang J, Wu D, Zhang Z, Li J, Shen Y, Wang Z, Li Y, Zhang ZY and Sun J: Biomimetically ornamented rapid prototyping fabrication of an apatite-collagen-polycaprolactone composite construct with nano-micro-macro hierarchical structure for large bone defect treatment. ACS Appl Mater Interfaces 7: 26244-26256, 2015.
6. Pilia M, Guda T and Appleford M: Development of composite scaffolds for load-bearing segmental bone defects. Biomed Res Int 2013: 458253, 2013.
7. Inzana JA, Olvera D, Fuller SM, Kelly JP, Graeve OA, Schwarz EM, Kates SL and Awad HA: 3D printing of composite calcium phosphate and collagen scaffolds for bone regeneration. Biomaterials 35: 4026-4034, 2014.
8. Papadimitropoulos A, Riboldi SA, Tonnarelli B, Piccinini E, Woodruff MA, Hutmacher DW and Martin I: A collagen network phase improves cell seeding of open-pore structure scaffolds under perfusion. J Tissue Eng Regen Med 7: 183-191, 2013.
9. Zein I, Hutmacher DW, Tan KC and Teoh SH: Fused deposition modeling of novel scaffold architectures for tissue engineering applications. Biomaterials 23: 1169-1185, 2002.
10. Siddiqui N, Asawa S, Birru B, Baadhe R and Rao S: PCL-based composite scaffold matrices for tissue engineering applications. Mol Biotechnol, 2018.
11. Kim W, Jang CH and Kim G: Optimally designed collagen/polycaprolactone biocomposites supplemented with controlled release of HA/TCP/rhBMP-2 and HA/TCP/PRP for hard tissue regeneration. Mater Sci Eng C Mater Biol Appl 78: 763-772, 2017.
12. Cui Z, Lin L, Si J, Luo Y, Wang Q, Lin Y, Wang X and Chen W: Fabrication and characterization of chitosan/OGP coated porous poly(epsilon-caprolactone) scaffold for bone tissue engineering. J Biomater Sci Polym Ed 28: 826-845, 2017.
13. Kiran S, Nune KC and Misra RD: The significance of grafting collagen on polycaprolactone composite scaffolds: Processing-structure-functional property relationship. J Biomed Mater Res A 103: 2919-2931, 2015.
14. Pek YS, Gao S, Arshad MS, Leck KJ and Ying JY: Porous collagen-apatite nanocomposite foams as bone regeneration scaffolds. Biomaterials 29: 4300-4305, 2008.
15. Xie C, Lu X, Han L, Xu J, Wang Z, Jiang L, Wang K, Zhang H, Ren F and Tang Y: Biomimetic mineralized hierarchical graphene oxide/chitosan scaffolds with adsorbability for immobilization of nanoparticles for biomedical applications. ACS Appl Mater Interfaces 8: 1707-1717, 2016.
16. Wang C, Zhao Q and Wang M: Cryogenic 3D printing for producing hierarchical porous and rhBMP-2-loaded Ca-P/PLLA nanocomposite scaffolds for bone tissue engineering. Biofabrication 9: 025031, 2017.
17. Yan Q, Xiao LQ, Tan L, Sun W, Wu T, Chen LW, Mei Y and Shi B: Controlled release of simvastatin-loaded thermo-sensitive PLGA-PEG-PLGA hydrogel for bone tissue regeneration: In vitro and in vivo characteristics. J Biomed Mater Res A 103: 3580-3589, 2015.
18. Papadimitriou K, Karkavelas G, Vouros I, Kessopoulou E and Konstantinidis A: Effects of local application of simvastatin on bone regeneration in femoral bone defects in rabbit. J Craniomaxillofac Surgy 43: 232-237, 2015.
19. Montero J, Manzano G and Albaladejo A: The role of topical simvastatin on bone regeneration: A systematic review. J Clin Exp Dent 6: e286-e290, 2014.
20. Tanigo T, Takaoka R and Tabata Y: Sustained release of water-insoluble simvastatin from biodegradable hydrogel augments bone regeneration. J Control Release 143: 201-206, 2010.
21. Park JB: The use of simvastatin in bone regeneration. Med Oral Patol Oral Cir Bucal 14: e485-e488, 2009.
22. Mir M, Ahmed N and Rehman AU: Recent applications of PLGA based nanostructures in drug delivery. Colloids Surf B Biointerfaces 159: 217-231, 2017.
23. Li H, Liao H, Bao C, Xiao Y and Wang Q: Preparation and evaluations of mangiferin-loaded PLGA scaffolds for alveolar bone repair treatment under the diabetic condition. AAPS Pharm Sci Tech 18: 529-538, 2017.
24. Hu X, Zhang J, Tang X, Li M, Ma S, Liu C, Gao Y, Zhang Y, Liu Y, Yu F, *et al*: An accelerated release method of risperidone loaded PLGA microspheres with good IVIVC. Curr Drug Deliv 15: 87-96, 2018.
25. Huang J, Chen Z, Li Y, Li Land Zhang G: Rifapentine-linezolid-loaded PLGA microspheres for interventional therapy of cavitary pulmonary tuberculosis: Preparation and in vitro characterization. Drug Des Devel Ther 11: 585-592, 2017.
26. Li Y, Zhang Z and Zhang Z: Porous chitosan/nano-hydroxyapatite composite scaffolds incorporating simvastatin-loaded PLGA microspheres for bone repair. Cells Tissues Organs 205: 20-31, 2018.
27. Fernández-Sánchez L, Bravo-Osuna I, Lax P, Arranz-Romera A, Maneu V, Esteban-Pérez S, Pinilla I, Puebla-González MDM, Herrero-Vanrell R and Cuenca N: Controlled delivery of tauroursodeoxycholic acid from biodegradable microspheres slows retinal degeneration and vision loss in P23H rats. PLoS One 12: e0177998, 2017.

28. Jeong C, Kim SE, Shim KS, Kim HJ, Song MH, Park K and Song HR: Exploring the in vivo anti-inflammatory actions of simvastatin-loaded porous microspheres on inflamed tenocytes in a collagenase-induced animal model of achilles tendinitis. Int J Mol Sci 19: E820, 2018.
29. Qiao F, Zhang J, Wang J, Du B, Huang X, Pang L and Zhou Z: Silk fibroin-coated PLGA dimpled microspheres for retarded release of simvastatin. Colloids Surf B Biointerfaces 158: 112-118, 2017.
30. Yu WL, Sun TW, Qi C, Zhao HK, Ding ZY, Zhang ZW, Sun BB, Shen J, Chen F, Zhu YJ, *et al*: Enhanced osteogenesis and angiogenesis by mesoporous hydroxyapatite microspheres-derived simvastatin sustained release system for superior bone regeneration. Sci Rep 7: 44129, 2017.
31. Li Y and Zhang ZZ: Sustained curcumin release from PLGA microspheres improves bone formation under diabetic conditions by inhibiting the reactive oxygen species production. Drug Des Devel Ther 12: 1453-1466, 2018.
32. Zhang W, Chang Q, Xu L, Li G, Yang G, Ding X, Wang X, Cui D and Jiang X: Graphene oxide-copper nanocomposite-coated porous CaP scaffold for vascularized bone regeneration via activation of Hif-1α. Adv Healthc Mater 5: 1299-1309, 2016.
33. Xie H, Wang Z, Zhang L, Lei Q, Zhao A, Wang H, Li Q, Cao Y, Jie Zhang W and Chen Z: Extracellular vesicle-functionalized decalcified bone matrix scaffolds with enhanced pro-angiogenic and pro-bone regeneration activities. Sci Rep 7: 45622, 2017.
34. Shen X, Zhang Y, Gu Y, Xu Y, Liu Y, Li B and Chen L: Sequential and sustained release of SDF-1 and BMP-2 from silk fibroin-nanohydroxyapatite scaffold for the enhancement of bone regeneration. Biomaterials 106: 205-216, 2016.
35. Li Y, Gao X and Wang J: Human adipose-derived mesenchymal stem cell-conditioned media suppresses inflammatory bone loss in a lipopolysaccharide-induced murine model. Exp Ther Med 15: 1839-1846, 2018.
36. Livak KJ and Schmittgen TD: Analysis of relative gene expression data using real-time quantitative PCR and the 2(-Delta Delta C(T)) method. Methods 25: 402-408, 2001.
37. National Research Council Committee for the Update of the Guide for the Care and Use of Laboratory Animals: The National Academies Collection: Reports funded by National Institutes of Health. In: Guide for the Care and Use of Laboratory Animals. th (ed). National Academies Press (US) National Academy of Sciences., Washington (DC), 2011.
38. Sun X, Wang J, Wang Y and Zhang Q: Collagen-based porous scaffolds containing PLGA microspheres for controlled kartogenin release in cartilage tissue engineering. Artif Cells Nanomed Biotechnol: 1-10, 2017.
39. Fahimipour F, Rasoulianboroujeni M, Dashtimoghadam E, Khoshroo K, Tahriri M, Bastami F, Lobner D and Tayebi L: 3D printed TCP-based scaffold incorporating VEGF-loaded PLGA microspheres for craniofacial tissue engineering. Dent Mater 33: 1205-1216, 2017.
40. Ramazani F, Chen W, van Nostrum CF, Storm G, Kiessling F, Lammers T, Hennink WE and Kok RJ: Strategies for encapsulation of small hydrophilic and amphiphilic drugs in PLGA microspheres: State-of-the-art and challenges. Int J Pharm 499: 358-367, 2016.
41. Giteau A, Venier-Julienne MC, Aubert-Pouëssel A and Benoit JP: How to achieve sustained and complete protein release from PLGA-based microparticles? Int J Pharm 350: 14-26, 2008.
42. Oryan A, Kamali A and Moshiri A: Potential mechanisms and applications of statins on osteogenesis: Current modalities, conflicts and future directions. J Control Release 215: 12-24, 2015.
43. Du L, Yang S, Li W, Li H, Feng S, Zeng R, Yu B, Xiao L, Nie HY and Tu M: Scaffold composed of porous vancomycin-loaded poly(lactide-co-glycolide) microspheres: A controlled-release drug delivery system with shape-memory effect. Mater Sci Eng C Mater Biol Appl 78: 1172-1178, 2017.
44. Guelcher SA, Brown KV, Li B, Guda T, Lee BH and Wenke JC: Dual-purpose bone grafts improve healing and reduce infection. J Orthop Trauma 25: 477-482, 2011.
45. Liu H, Yang L, Zhang E, Zhang R, Cai D, Zhu S, Ran J, Bunpetch V, Cai Y, Heng BC, *et al*: Biomimetic tendon extracellular matrix composite gradient scaffold enhances ligament-to-bone junction reconstruction. Acta Biomater 56: 129-140, 2017.
46. Du Y, Liu H, Yang Q, Wang S, Wang J, Ma J, Noh I, Mikos AG and Zhang S: Selective laser sintering scaffold with hierarchical architecture and gradient composition for osteochondral repair in rabbits. Biomaterials 137: 37-48, 2017.
47. Amini AR, Wallace JS and Nukavarapu SP: Short-term and long-term effects of orthopedic biodegradable implants. J Long Term Eff Med Implants 21: 93-122, 2011.
48. Nezu T and Winnik FM: Interaction of water-soluble collagen with poly(acrylic acid). Biomaterials 21: 415-419, 2000.
49. Hollister SJ: Porous scaffold design for tissue engineering. Nat Mater 4: 518-524, 2005.